

Abstract

Here we outline the progress of a study to construct infra-red exoplanet transmission spectra from opacity tables. We outline the various steps involved in doing so, from raw molecular line lists to planetary radii as a function of wavelength for a range of pressures and temperatures encountered on hot Jupiters.

Introduction

The study of exoplanet atmospheres is hinged upon the measurement of a transmission spectrum. When an exoplanet passes in front of its host star (passing through the line-of-sight of the observer) it causes a temporary drop in brightness known as a transit light curve. If the planet has some kind of atmospheric component then R_p will change depending on the constituents of the atmosphere. For instance, if the planet has a large amount of potassium in its atmosphere and you observe a transit at λ where potassium has strong absorption features ($\sim 7680\text{\AA}$) then the radius will appear larger to the observer due to the relative increase in size of the observed opaque planetary body at that λ , $R_p(\lambda)$. For alkali metals such as sodium and potassium there are some extremely clear and relatively isolated absorption features that dominate the visual part of the spectrum. Unfortunately as we move to the IR spectral region numerous molecular species become strong absorbers in the wide range of high temperatures (up to $\sim 3000\text{K}$) present on hot Jupiters such as methane, carbon monoxide, water and ammonia.

$$S_{ij} = \frac{g_j A_{ij}}{8\pi c \tilde{\nu}_0^2} \frac{e^{-hcE_i/k_B T}}{Q(T)} \left[1 - e^{-hc\tilde{\nu}_0/k_B T} \right]$$

The strength [cm/species] of the transition from states i - j at a wavenumber of ν_0 is a function of the degeneracy (g), Einstein A coefficient, lower state energy (E) and atmospheric temperature (T). Scaling the intensity with temperature is relatively simple if $Q(T)$ is scaled correctly.

There are two main broadening mechanisms in the P - T range of interest:

-*Doppler*: due to motion of the absorbing species w.r.t. the observer. It has a Gaussian form and is proportional to $T^{1/2}$.

-*Pressure*: a result of collisions with the absorber and other atmospheric species and can be decomposed into foreign and self components. It has a Lorentzian shape and is proportional to PT^n .

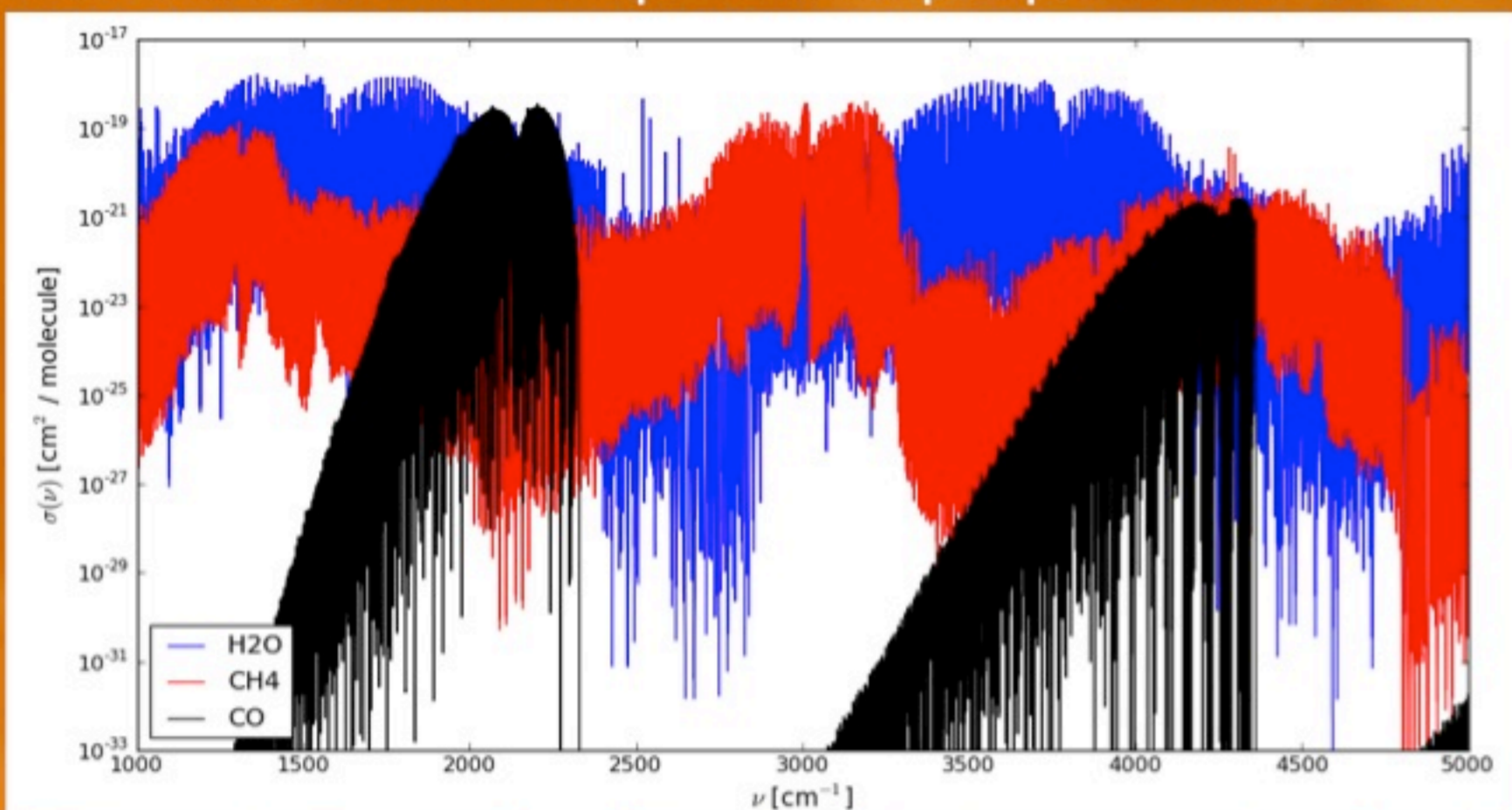


Figure 1: Example absorption cross-section for CO using $P=0.01\text{atm}$ and $T=1500\text{K}$. CH_4 and H_2O are shown for comparison but from a much sparser line list than those described above.

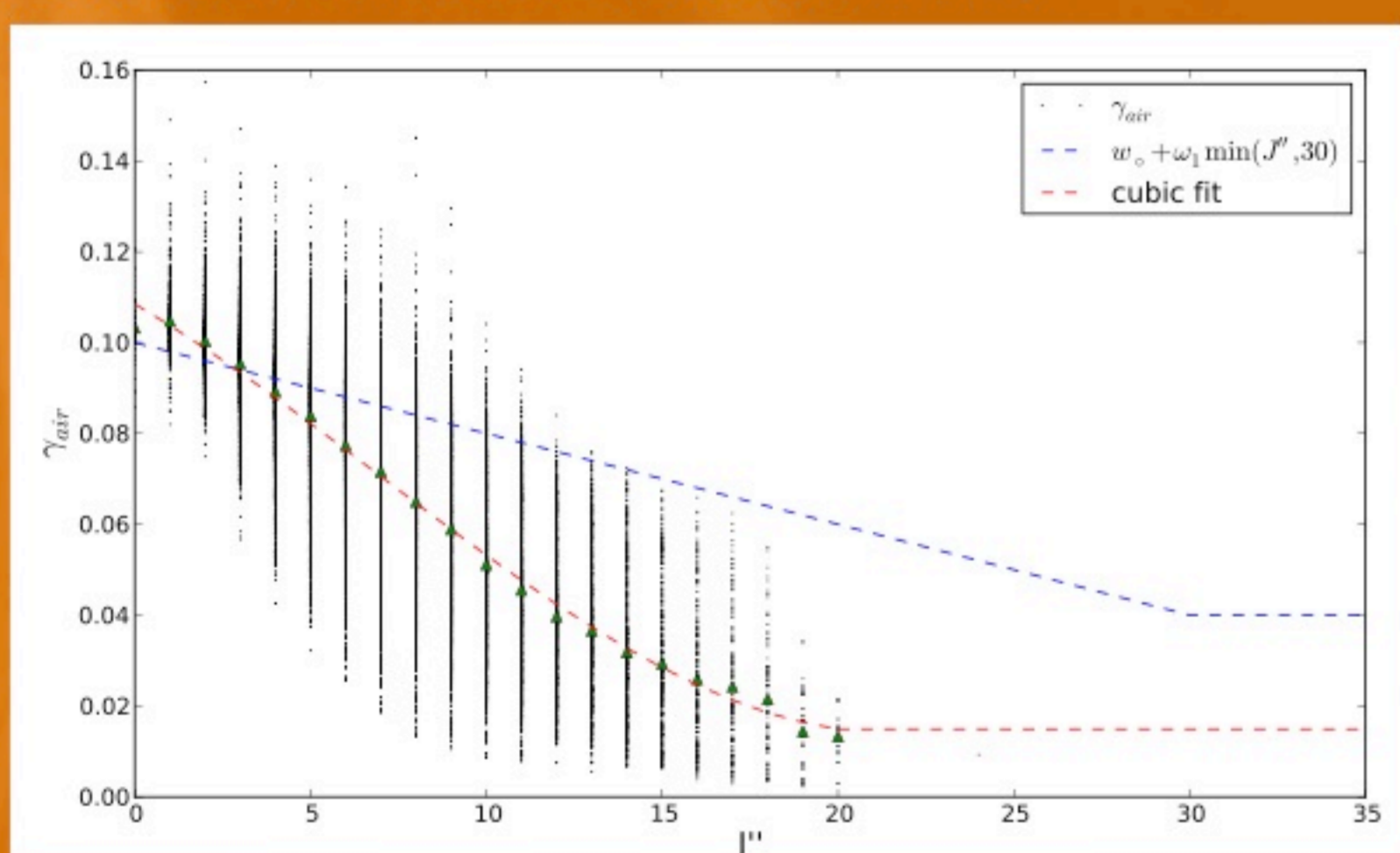


Figure 2: Extrapolation of air-broadening coefficient for H_2O as a function of J'' (red line), with a basic species-wide fit for comparison (blue line).

Some of the lines in high temperature databases lack the broadening coefficients needed to form a profile. In this case we fit coefficients as a function of J'' (rotational quantum number of the lower state) as in Fig. 2 and use this to estimate the unknown values.

Line Lists

The first step in building a transmission spectrum is obtaining the list of molecular line transitions that will contribute to the overall opacity of the atmosphere. There are several different line databases available but not all are suitable for the high temperatures found on hot Jupiters (those we use are summarised to the right).

The higher the temperatures we require, the more line transitions become possible. This results in line lists that are millions of lines long making the choice of wavenumber (ν) resolution and broadening distance crucial.

Species	Source	# Lines	Range [cm^{-1}]
H_2O	HITEMP (a.k.a. BT2)	111,377,777	0 - 30,000
CH_4	Boudon(*)/ HITRAN	5,001,575 + 34,536	0 - 9,200
CO	HITEMP/ GEISA	113,294 + 3,442	0 - 8,465
NH_3	BYTe	1,138,323,351	0 - 12,000

*Our CH_4 lines come from Boudon et al. 2011: <http://vamdc.icb.cnrs.fr/PHP/methane.php>

Broadening

Once the lines have been gathered and scaled to the temperature of interest their intensity must then be broadened by some appropriate profile (ϕ , cm) resulting from some physical effect. This results in the absorption cross section, σ , for the species of interest at a certain P - T . This is then summed across all species.

$$\sigma(\nu, T, P) = S(T) \phi(\nu, T, P)$$

Transmission

Now σ has been tabulated we follow the analytic model of Lecavelier Des Etangs et al. 2006 to find the change in planetary radius as a function of wavelength. τ_{eq} is the optical depth of the original planetary radius and is assumed to be approximately constant (0.56).

$$R_p(\nu) = R_{p,\phi} + \frac{k_B T}{\mu g} \ln \left[\frac{\xi P_\phi \sigma(\nu)}{\tau_{eq}} \sqrt{\frac{2\pi R_{p,\phi}}{k_B T \mu g}} \right]$$

Correlated-k

The correlated-k method is based on the derivation of probability density distributions of the absorption coefficient strengths from line-by-line calculations. It is two to three orders of magnitude faster than line-by-line calculations and is easily propagated to new P - T coordinates.

Partition Functions

The strength of a line transition will change with the temperature of the surrounding medium. The partition function, $Q(T)$, present in the equation for line strength is also temperature dependant. It can be either calculated directly from the occupation of molecular states or extrapolated with a power law fit.

$$Q(T) = \sum_{i=1}^n g_i e^{-hcE_i/k_B T}$$

We use the information from Barber et al. 2006, Yurchenko et al. 2011, Wenger et al. 2008 and Rothman et al. 2009 (H_2O , NH_3 , CH_4 and CO respectively) to evaluate $Q(T)$.

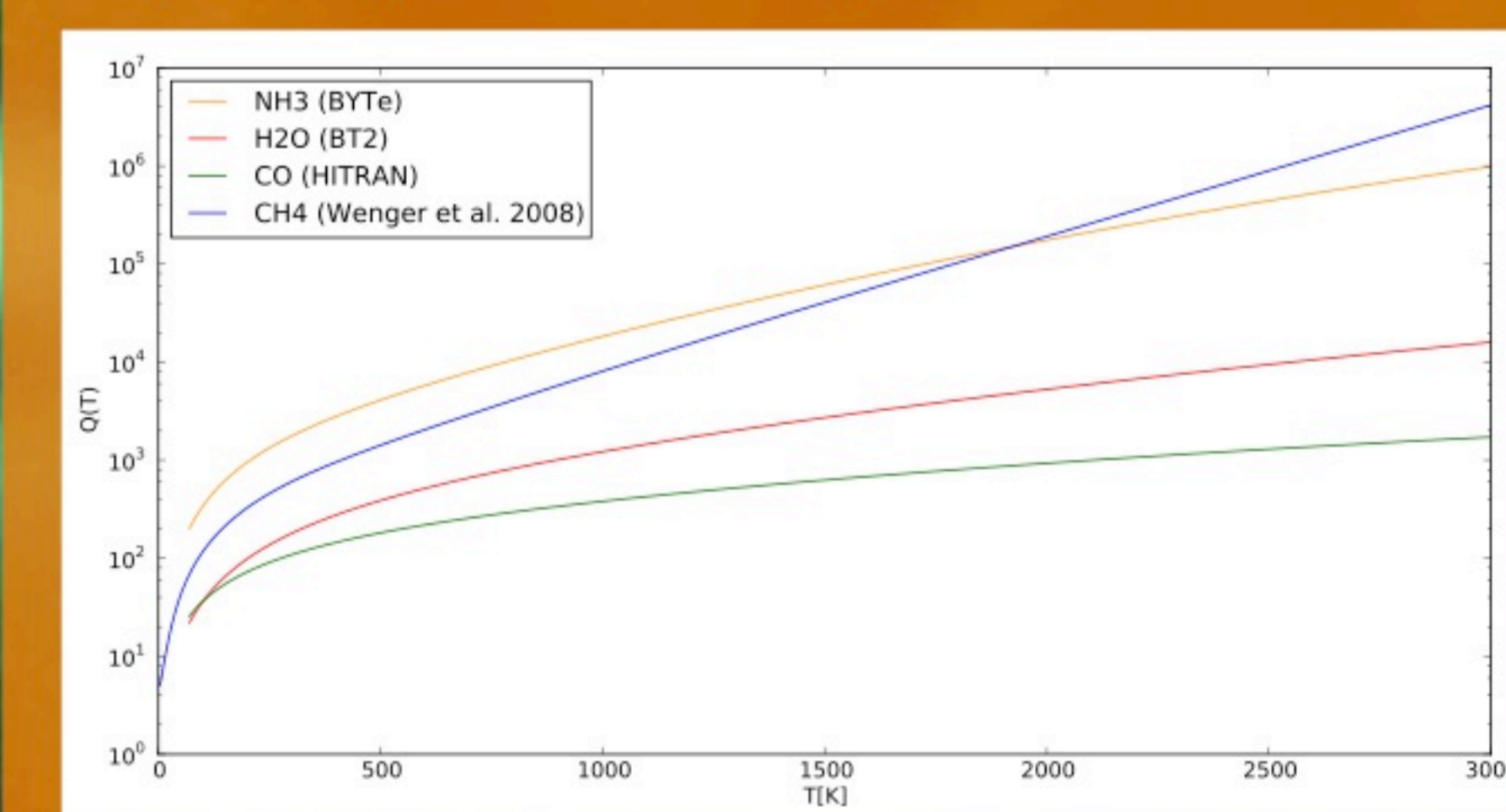


Figure 3: Partition functions over our P - T range of interest for species important in the IR.

Everything else...

There are other physical processes apart from molecular line transitions that contribute to the total opacity. This includes collision induced absorption and grain opacities (Rayleigh/Mie scattering). Our treatment of which will follow that of Sharp & Burrows 2007.

The relative abundances of the various species (as a function of P - T) must also be known, and this in turn depends on the P - T profile used.

References

- Barber, R. J., Tennyson, J., Harris, G. J., & Tolchenov, R. N. 2006, MNRAS (BT2 list)
- Boudon, V., et al. 2011, EPSC-DPS2011-115, Vol. 6 (CH_4 list)
- Jacquinet-Husson, N., et al. 2011, JQSRT, 112, 2395 (GEISA list)
- Lecavelier Des Etangs, A., Pont, F., Vidal-Madjar, A., & Sing, D. 2008, A & A, 481, L83
- Rothman, L., et al. 2009, JQSRT, 110, 533 (HITRAN list)
- Rothman, L., et al. 2010, JQRST, 111, 2139 (HITEMP list)
- Sharp, C. M., & Burrows, A. 2007, ApJS, 168, 140
- Wenger, C., Champion, J., & Boudon, V. 2008, JQRST, 109, 2697
- Yurchenko, S. N., Barber, R. J., & Tennyson, J. 2011, MNRAS, 413, 1828 (BYTe list)
- Burge P., background artwork: <http://www.chronoscapes.com/> retrieved 18/03/12